

# The Crystal Structure of an Azide Complex of the Diferrous R2 Subunit of Ribonucleotide Reductase Displays a Novel Carboxylate Shift with Important Mechanistic Implications for Diiron-Catalyzed Oxygen Activation

Martin E. Andersson,<sup>‡,¶</sup> Martin Högbom,<sup>‡,¶</sup> Agnes Rinaldo-Matthis,<sup>‡,¶</sup>  
K. Kristoffer Andersson,<sup>†</sup> Britt-Marie Sjöberg,<sup>‡</sup> and Pär Nordlund<sup>\*,‡,¶</sup>

Contribution from the Department of Biochemistry, Stockholm University, S-106 91 Stockholm, Sweden, Department of Biochemistry, University of Oslo, P.O. Box 1041, Blindern, N-0316 Oslo, Norway, and Department of Molecular Biology, Stockholm University, S-106 91 Stockholm, Sweden

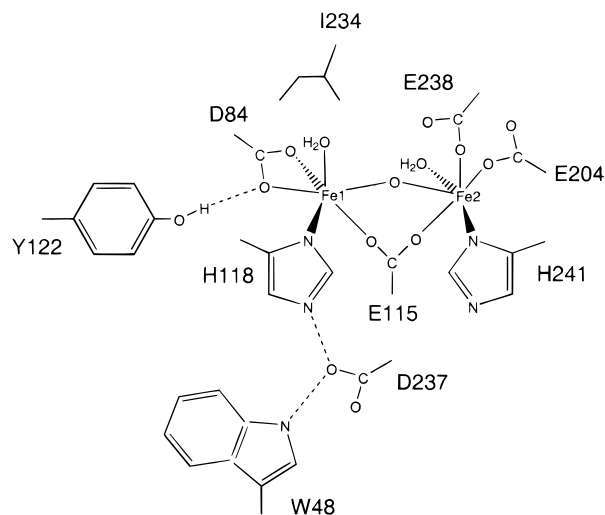
Received June 29, 1998

**Abstract:** The dinuclear Fe-center in the R2 protein of ribonucleotide reductase catalyzes oxygen activation chemistry leading to generation of the essential stable tyrosyl radical. Related oxygen reactions occur in several other diiron-containing enzyme systems where highly oxidative reaction intermediates are required to activate the substrates. Two such examples are methane monooxygenase and  $\Delta^9$  stearoyl-acyl carrier protein desaturase where oxygen activation takes place at Fe-centers whose structures are similar to the Fe-center in R2. In an attempt to structurally characterize the nature of the dioxygen cleavage reaction performed by these proteins we have determined the crystal structures of two different forms of the diferrous R2 protein in the presence of azide, a potential Fe ligand. In crystals of the wt protein no azide binding was detected. The mutant protein F208A/Y122F has a larger hydrophobic pocket around the Fe-center and in the structure of this protein azide bind as an  $\eta^1$ -terminal ligand to Fe2, the Fe ion farthest away from the tyrosine residue to be oxidized in the radical generation reaction. Glu 238, the Fe ligand most exposed into the hydrophobic pocket, coordinates the Fe-center in a novel  $\mu$ -( $\eta^2, \eta^1$ ) bridging mode with one of the carboxylate oxygen atoms forming a bridge between the two iron ions and the other oxygen being coordinated to Fe2. Through this bridging the Fe–Fe distance is shortened to about 3.4 Å as compared to 3.9 Å for the structure of the reduced wt protein. On the basis of the novel carboxylate shift and recent data on the spectroscopic properties of the key intermediate X we propose a unique structure for intermediate X and a detailed mechanism for dioxygen cleavage. This mechanism suggests an asymmetric oxygen cleavage with a terminal oxo/hydroxo group as the major species responsible for substrate activation.

## Introduction

The R2 protein of ribonucleotide reductase (RNR) from *E. coli* contains a  $\mu$ -oxo bridged dinuclear iron center coordinated by carboxylate and histidine residues<sup>1</sup> (Scheme 1). This Fe-center is essential for generation and stabilization of the tyrosyl radical needed for the reduction of ribonucleotides to deoxyribonucleotides performed by this enzyme.<sup>2–6</sup> The ribonucleotide substrates are bound to the R1 subunit<sup>7</sup> to which the radical is transferred to initiate the substrate reduction reaction. Transfer of the radical between R2 and R1 during catalysis has been proposed to occur via an array of conserved amino acids that form a hydrogen-bonded path, connecting the tyrosyl radical

**Scheme 1.** The Fe-Center in RNR R2<sup>a</sup>



<sup>a</sup> The ligands to the Fe-center, the radical-harboring tyrosine 122, part of the hydrophobic pocket (I234), and the coupled proton/electron transfer pathway (D237 and W48) are shown.

in R2 with the active site in R1.<sup>1,8,9</sup> This proposed radical-transfer pathway is not only important for radical transfer to

\* To whom correspondence should be addressed.

† Department of Biochemistry, Stockholm University.

‡ Department of Biochemistry, University of Oslo.

§ Department of Molecular biology, Stockholm University.

(1) Nordlund, P.; Sjöberg, B.-M.; Eklund, H. *Nature* **1990**, *345*, 593–598.

(2) Sjöberg, B. M. *Struct. Bonding* **1997**, *88*, 139–173.

(3) Stubbe, J.; van der Donk, W. *Chem. Biol.* **1995**, *2*, 793–801.

(4) Gräslund, A.; Sahlin, M. *Annu. Rev. Biophys. Biomol. Struct.* **1996**, *25*, 259–86.

(5) Andersson, K. K.; Gräslund, A. *Adv. Inorg. Chem.* **1995**, *43*, 359–409.

(6) Fontecave, M.; Nordlund, P.; Eklund, H.; Reichard, P. *Adv. Enzymol. Relat. Areas Mol. Biol.* **1992**, *65*, 147–83.

(7) Reichard, P. *Science* **1993**, *260*, 1773–1777.

**Table 1.** The Various Intermediates Isolated in R2 and MMO and Their Key Features

R2	redox state of diiron core	MMO
Red	Fe <sup>2+</sup> Fe <sup>2+</sup>	Red
(P)	oxygen complex Fe <sup>2+</sup> Fe <sup>2+</sup> peroxide complex Fe <sup>3+</sup> Fe <sup>3+</sup>	O P
X	Fe <sup>4+</sup> Fe <sup>4+</sup> Fe <sup>3+</sup> Fe <sup>4+</sup>	Q
	substrate radical complex Fe <sup>3+</sup> Fe <sup>4+</sup> enzyme-product complex Fe <sup>3+</sup> Fe <sup>3+</sup>	R T
active	Tyr radical, Fe <sup>3+</sup> Fe <sup>3+</sup>	
Met	Fe <sup>3+</sup> Fe <sup>3+</sup>	H <sub>ox</sub>

the R1 subunit<sup>1,10–13</sup> but is also essential in the radical generation reaction.<sup>14–17</sup>

Radical generation occurs when the reduced diiron center in the R2 protein reacts with dioxygen. The oxygen molecule is cleaved to generate high-valent Fe intermediates that oxidize the Y122, producing the essential radical. To fully reduce dioxygen and generate the diferric, radical-containing protein, one proton and one electron are supplied via the radical transfer pathway. Other enzyme systems use similar Fe-centers to perform other kinds of dioxygen dependent redox chemistry. Methane monooxygenase (MMO)<sup>18</sup> and  $\Delta^9$  stearoyl-acyl carrier protein desaturase ( $\Delta^9$  desaturase)<sup>19,20</sup> are two examples both using dioxygen to generate highly activated diiron sites. The R2 protein was the first protein with this type of Fe-center to be studied by X-ray crystallography.<sup>1</sup> Later studies of the crystal structures of MMO<sup>21</sup> and  $\Delta^9$  desaturase<sup>20</sup> confirmed that the Fe-center environments in these proteins have many similarities.

Time-resolved spectroscopic techniques have allowed the isolation and characterization of several reaction intermediates in the dioxygen activation reaction (Table 1). The only relatively well-characterized intermediate isolated in the wild-type R2 system is intermediate X,<sup>22–25</sup> having a formally Fe<sup>III</sup>–Fe<sup>IV</sup> center with an Fe–Fe distance of about 2.5 Å. This intermediate is proposed to be the precursor to the tyrosyl radical containing diferric species. MMO is the system that has allowed the

observation of the highest number of intermediates (Table 1). For a recent review, see ref 18. The reaction cycle starts when the diferrous Fe-center binds one molecule of oxygen. The first suggested intermediate in the MMO reaction, termed O, is thought to consist of an oxygen molecule bound at or near the diferrous Fe-center.<sup>26</sup> The next intermediate formed, called P, has been interpreted as being a peroxide bound to the diferric Fe-center.<sup>27</sup> After O–O bond cleavage an intermediate termed Q is formed.<sup>28,29</sup> The spectroscopic characteristics of this intermediate have led to suggestions that it has an Fe<sup>IV</sup>–O<sub>2</sub> “diamond core” structure with a short Fe–Fe distance of about 2.46 Å.<sup>29</sup> Intermediate Q is the activated form of the enzyme, which is believed to react with substrate. Despite extensive kinetic, structural, and spectroscopic studies, a detailed understanding of the mechanism of O<sub>2</sub> activation and substrate oxidation by diiron sites is still missing. Several mechanisms for dioxygen cleavage have been suggested, but the lack of information regarding the initial O<sub>2</sub> binding makes it difficult to determine which of these is the most likely reaction path.<sup>30–35</sup> Our goal was to study the earliest steps of this reaction using small-molecule ligands. These ligands might mimic oxygen binding and thereby define possible O<sub>2</sub> interactions with the Fe-center and map structural changes at the Fe-center that could be induced by O<sub>2</sub> binding. In diferrous R2 and related proteins the azide complex formed in the presence of high concentrations of azide induce ferromagnetically coupled iron as observed by EPR, MCD, and magnetic susceptibility measurements.<sup>36–38</sup> This is probably due to direct binding of azide to the iron cluster as indicated by integer spin ESEEM and MCD studies.<sup>37,39</sup>

The availability of high-resolution crystal structures of several forms of the R2 protein and the possibility of directed mutagenesis and high overexpression of recombinant protein makes this system a particularly good candidate as a model system to study the oxygen activation mechanism. In this work we have used X-ray crystallographic methods to investigate the binding of azide to the diferrous centers of the wild-type form as well as one mutant form of the R2 protein. The mutant used was F208A/Y122F, which was expected to have an unusually accessible Fe-center to allow a high level of ligand binding. A novel carboxylate shift was found which gave important information for understanding the mechanism of dioxygen activation.

The structure of the oxidized form of the F208A/Y122F mutant was also determined and showed no significant changes

(8) Uhlin, U.; Eklund, H. *Nature* **1994**, *370*, 533–539.

(9) Sjöberg, B.-M. *Structure* **1994**, *2*, 793–796.

(10) Climent, I.; Sjöberg, B. M.; Huang, C. Y. *Biochemistry* **1992**, *31*, 4801–7.

(11) Rova, U.; Goodtzova, K.; Ingemarson, R.; Behravan, G.; Gräslund, A.; Thelander, L. *Biochemistry* **1995**, *34*, 4267–75.

(12) Ekberg, M.; Pötsch, S.; Sandin, E.; Thunnissen, M.; Nordlund, P.; Sahlin, M.; Sjöberg, B. M. *J. Biol. Chem.* **1998**, *273*, 21003–8.

(13) Ekberg, M.; Sahlin, M.; Eriksson, M.; Sjöberg, B. M. *J. Biol. Chem.* **1996**, *271*, 20655–20659.

(14) Sahlin, M.; Lassmann, G.; Pötsch, S.; Slaby, A.; Sjöberg, B. M.; Gräslund, A. *J. Biol. Chem.* **1994**, *269*, 11699–702.

(15) Sahlin, M.; Lassmann, G.; Pötsch, S.; Sjöberg, B. M.; Gräslund, A. *J. Biol. Chem.* **1995**, *270*, 12361–72.

(16) Schmidt, P. P.; Rova, U.; Katterle, B.; Thelander, L.; Gräslund, A. *J. Biol. Chem.* **1998**, *273*, 21463–72.

(17) Parkin, S. E.; Shuxian, C.; Ley, B. A.; Mangravite, L.; Edmondson, D. E.; Huynh, B. H.; Bollinger, J. M. *Biochemistry* **1998**, *37*, 1124–1130.

(18) Wallar, B. J.; Lipscomb, J. D. *Chem. Rev.* **1996**, *96*, 2625–2657.

(19) Fox, B. G.; Shanklin, J.; Ai, J.; Loehr, T. M.; Sanders-Loehr, J. *Biochemistry* **1994**, *33*, 12776–86.

(20) Lindqvist, Y.; Huang, W. J.; Schneider, G.; Shanklin, J. *EMBO J.* **1996**, *15*, 4081–4092.

(21) Rosenzweig, A. C.; Frederick, C. A.; Lippard, S. J.; Nordlund, P. *Nature* **1993**, *366*, 537–543.

(22) Bollinger, J. M.; Edmondson, D. E.; Huynh, B. H.; Filley, J.; Norton, J. R.; Stubbe, J. *Science* **1991**, *253*, 292–298.

(23) Sturgeon, B. E.; Burdi, D.; Chen, S.; Huynh, B. H.; Edmondson, D. E.; Stubbe, J.; Hoffman, B. M. *J. Am. Chem. Soc.* **1996**, *118*, 7551–7557.

(24) Willems, J. P.; Lee, H. I.; Burdi, D.; Doan, P. E.; Stubbe, J.; Hoffman, B. M. *J. Am. Chem. Soc.* **1997**, *119*, 9816–9824.

(25) Riggs-Gelasco, P. J.; Shu, L. J.; Chen, S. X.; Burdi, D.; Huynh, B. H.; Que, L.; Stubbe, J. *J. Am. Chem. Soc.* **1998**, *120*, 849–860.

(26) Liu, Y.; Nesheim, J. C.; Lee, S. K.; Lipscomb, J. D. *J. Biol. Chem.* **1995**, *270*, 24662–5.

(27) Liu, K. E.; Valentine, A. M.; Qui, D.; Edmondson, D. E.; Appelman, E. H.; Spiro, T. G.; Lippard, S. J. *J. Am. Chem. Soc.* **1995**, *117*, 4997–4998.

(28) Lee, S. K.; Fox, B. G.; Froland, W. A.; Lipscomb, J. D.; Münck, E. *J. Am. Chem. Soc.* **1993**, *115*, 6450–6451.

(29) Shu, L. J.; Nesheim, J. C.; Kauffmann, K.; Munck, E.; Lipscomb, J. D.; Que, L. *Science* **1997**, *275*, 515–518.

(30) Deeth, R. J.; Dalton, H. *J. Biol. Inorg. Chem.* **1998**, *3*, 302–306.

(31) Whittington, D. A.; Valentine, A. M.; Lippard, S. J. *J. Biol. Inorg. Chem.* **1998**, *3*, 307–313.

(32) Siegbahn, P. E. M.; Crabtree, R. H.; Nordlund, P. *J. Biol. Inorg. Chem.* **1998**, *3*, 314–317.

(33) Yoshizawa, K. *J. Biol. Inorg. Chem.* **1998**, *3*, 318–324.

(34) Shteinman, A. A. *J. Biol. Inorg. Chem.* **1998**, *3*, 325–330.

(35) Lipscomb, J. D.; Que, L. *J. Biol. Inorg. Chem.* **1998**, *3*, 331–336.

(36) Elgren, T. E.; Hendrich, M. P.; Que, L. *J. Am. Chem. Soc.* **1993**, *115*, 9291–9292.

(37) Pulver, S. C.; Tong, W. H.; Bollinger, J. M.; Stubbe, J.; Solomon, E. I. *J. Am. Chem. Soc.* **1995**, *117*, 12664–12678.

(38) Atta, M.; Debaecker, N.; Andersson, K. K.; Latour, J. M.; Thelander, L.; Gräslund, A. *J. Biol. Inorg. Chem.* **1996**, *1*, 210–220.

(39) Sturgeon, B. E.; Doan, P. E.; Liu, K. E.; Burdi, D.; Tong, W. H.; Nocek, J. M.; Gupta, N.; Stubbe, J.; Kurtz, D. M.; Lippard, S. J.; Hoffman, B. M. *J. Am. Chem. Soc.* **1997**, *119*, 375–386.

in coordination of the Fe-center, or other structural changes except for the large hydrophobic pocket formed by the removal of the F208 side-chain which makes the Fe-center more accessible to small-molecule ligands.

## Experimental Section

**Mutagenesis and Protein Preparation.** All chemicals were purchased from Sigma. BsiWI restriction enzyme was from New England Biolabs. The vector used for expressing F208A/Y122F mutant was constructed from the plasmid pMK5<sup>40</sup> according to the MUTA-GENE Phagemid in vitro mutagenesis kit (Bio-Rad Laboratories). The primer used in the mutagenesis reaction had the sequence 5'-AAG CGA TTC GTG **CGT ACG TCA GC**-3' and was purchased from Scandinavian Gene Synthesis. The bold letters indicate bases that differ from the wt-sequence. These bases were mutagenized to introduce the desired amino acid substitution and to generate a new restriction site for the enzyme BsiWI (underlined) to facilitate screening for mutant colonies. After transformation of *E. coli* with the mutagenesis mixture, bacterial colonies were suspended in water and the mutagenized R2 gene was amplified by using the DNA Thermal cycler (Perkin-Elmer) with the primers Universal and Reverse (Pharmacia). The PCR products were cleaved with the BsiWI enzyme and analyzed on an agarose gel to detect mutant colonies (data not shown). Overexpression and purification of wt and mutant R2 proteins were done according to standard methods for the wt-enzyme.<sup>41</sup> The wt- and the F208A/Y122F mutant-proteins were prepared as Fe-containing proteins. The integrity of the Fe-center and the expected absence of tyrosyl radical in the F208A/Y122F mutant were confirmed with UV/vis light absorption spectroscopy (data not shown). The wavelength range used was 250–750 nm on a Lambda2 UV/VIS spectrophotometer (Perkin-Elmer).

**Protein Crystallization and Crystal Soaking.** Protein crystals were grown by using the hanging drop method as described previously.<sup>42</sup> The crystals belong to space group  $P2_12_12_1$  and attained a size of about  $0.5 \times 0.2 \times 0.2$  mm.

When Fe-containing crystals are grown in this way the Fe-center is always in its met form upon crystallization. To reduce the Fe-center the wt crystals were soaked in N<sub>2</sub>-flushed mother liquor supplemented with 0.5% Na-dithionite and 1 mM phenosafranin. Reaction volumes were 1 mL in Falcon tissue culture plates sealed with a glass cover slip. The wt crystals were soaked for 90 min in this solution. To keep the Fe-center reduced while binding azide, the crystals were soaked in N<sub>2</sub>-flushed mother liquor supplemented with 0.5% Na-dithionite and 500 mM NaN<sub>3</sub> for 30 min. The crystals were transferred to mother liquor with 20% glycerol as cryoprotectant, 0.5% Na-dithionite, and 500 mM NaN<sub>3</sub> and soaked for 1–2 min. Crystals were picked up in rayon loops (Hampton Research) and flash frozen in liquid N<sub>2</sub>.

For the F208A/Y122F crystals the Fe-center was reduced and azide was bound in a soak with mother liquor containing 3% Na-dithionite, 1 mM phenosafranin, and 500 mM NaN<sub>3</sub> for 75 min. The freezing procedure was the same as in the wt experiment, except for the Na-dithionite concentration that was 3% in this case.

**Data Collection and Refinement.** Diffraction data for the azide-soaked crystals were collected at the Swiss-Norwegian beam-line at the European Synchrotron Radiation Facility (ESRF), Grenoble, France. The beam line was equipped with a 30 cm imaging plate (Mar Research) and a cryosystem (Oxford cryosystems). The wavelength used was 1.00 Å for both data sets. For the oxidized F208A/Y122F protein, diffraction data were collected on a MarResearch imaging plate mounted on a Siemens rotating anode. The wavelength used was 1.54 Å and the crystal was frozen with a Siemens LC2 cryosystem. For details on data collection and refinement, see Table 2. The Denzo and Scalepack<sup>43</sup> programs were used for processing and scaling of the diffraction data.

(40) Karlsson, M.; Sahlin, M.; Sjöberg, B. M. *J. Biol. Chem.* **1992**, *267*, 12622–12626.

(41) Sjöberg, B.-M.; Hahne, S.; Karlsson, M.; Jörnval, H.; Göransson, M.; Uhlin, B. E. *J. Biol. Chem.* **1986**, *261*, 5658–5662.

(42) Nordlund, P.; Uhlin, U.; Westergren, C.; Joelsen, T.; Sjöberg, B. M.; Eklund, H. *FEBS Lett.* **1989**, *258*, 251–254.

(43) Otwinowski, Z. *Data collection and processing. Proceedings of the CCP4 study weekend*; SERC Daresbury Laboratory: Warrington, U.K., 1993; pp 56–62.

**Table 2.** Data Collection and Refinement Statistics

data set	F208A/Y122F azide	F208A/Y122F	WT azide
data			
cell parameters			
<i>a</i> (Å)	73.8	73.9	73.9
<i>b</i> (Å)	84.2	83.2	84.9
<i>c</i> (Å)	113.5	113.4	114.2
space group	P2 <sub>1</sub> 2 <sub>1</sub> 2 <sub>1</sub>	P2 <sub>1</sub> 2 <sub>1</sub> 2 <sub>1</sub>	P2 <sub>1</sub> 2 <sub>1</sub> 2 <sub>1</sub>
resolution (Å)	25–2.0	20–2.4	20–2.4
no. of observations	144767	138917	91571
unique reflns	43085	24934	28207
<i>R</i> <sub>merge</sub> <sup>a</sup>	0.063	0.101	0.098
completeness (%)	88.7	88.7	94.8
refinement			
non-H atoms	5925	5851	5902
<i>R</i> <sub>cryst</sub> <sup>b</sup>	0.197	0.181	0.194
reflns used	40931	22412	26797
<i>R</i> <sub>free</sub> <sup>c</sup>	0.289	0.262	0.290
reflns used	2154	2522	1410
<i>R</i> <sub>cryst</sub> (all data) <sup>b</sup>	0.197	0.181	0.194
mean <i>B</i> factor (Å <sup>2</sup> )	39.2	36.2	33.8
rmsd from ideal			
bond length (Å)	0.020	0.007	0.014
bond angles (deg)	1.6	1.5	1.2

<sup>a</sup>  $R_{\text{merge}} = \sum_j \sum_h |I_{hj} - \bar{I}_h| / \sum_j \sum_h I_{hj}$  where  $I_{hj}$  is the  $j$ th observation of reflection  $h$ . <sup>b</sup>  $R_{\text{cryst}} = \sum |F_{\text{obs}} - F_{\text{calc}}| / \sum |F_{\text{obs}}|$ , where  $F_{\text{obs}}$  and  $F_{\text{calc}}$  are the observed and calculated structure factor amplitudes, respectively. <sup>c</sup>  $R_{\text{free}}$  is equivalent to  $R_{\text{cryst}}$  for a 5% subset of reflections not used in the refinement.

Refinement of the structures was performed with TNT.<sup>44</sup> The structures were solved with molecular replacement methods, using the structure of reduced wt R2 protein<sup>45</sup> with solvent molecules as a starting model. During the initial rounds of refinement the starting model was used as a rigid body and the resolution limits were gradually increased to the final values. Electron density maps were calculated with TNT and programs from the CCP4<sup>46</sup> suite. Interpretation of maps and model building was done with QUANTA (Molecular Simulations). During the progression of the positional refinement, water molecules with *B* factors > 70 Å<sup>2</sup> were removed and new waters added at peaks > 4σ in the Fo–Fc maps in several cycles. Progress of the refinement was monitored by using the free *R*-value,<sup>47</sup> using 5% of the data as a test set. Once the refinements had converged one last round of refinement was made with all the data included. For the wt data-set refinement was continued until it was evident that no azide was bound to the Fe-center in any of the subunits.

## Results and Discussion

In this paper we describe the X-ray crystal structures of two different forms of the diferrous R2 protein soaked in azide. In the F208A/Y122F mutant azide binds to the Fe-center in one of the subunits in the R2 dimer. This is the first crystal structure of an azide complex of a diferrous protein of this class. We also determined the structure of the oxidized F208A/Y122F, which revealed that the removal of the F208 side chain creates a larger hydrophobic cavity around the Fe-center while leaving the rest of the protein unchanged.

**Structure of the wt- and F208A/Y122F-Protein in the Presence of Azide.** From Fo–Fc maps it was evident that the wt protein did not have any azide bound to the Fe-center in any of the two noncrystallographically related subunits (A and B) in the R2 dimer. Both sites had the normal structure and coordination of diferrous R2 (Figure 1a).

(44) Tronrud, D. E. *Methods Enzymol.* **1997**, *277*, 306–319.

(45) Logan, D. T.; Su, X. D.; Åberg, A.; Regnström, K.; Hajdu, J.; Eklund, H.; Nordlund, P. *Structure* **1996**, *4*, 1053–1064.

(46) Collaborative computational project, no. 4: *Acta Crystallogr. C* **1994**, *50*, 760–763.

(47) Brünger, A. *Nature* **1992**, *355*, 472–475.

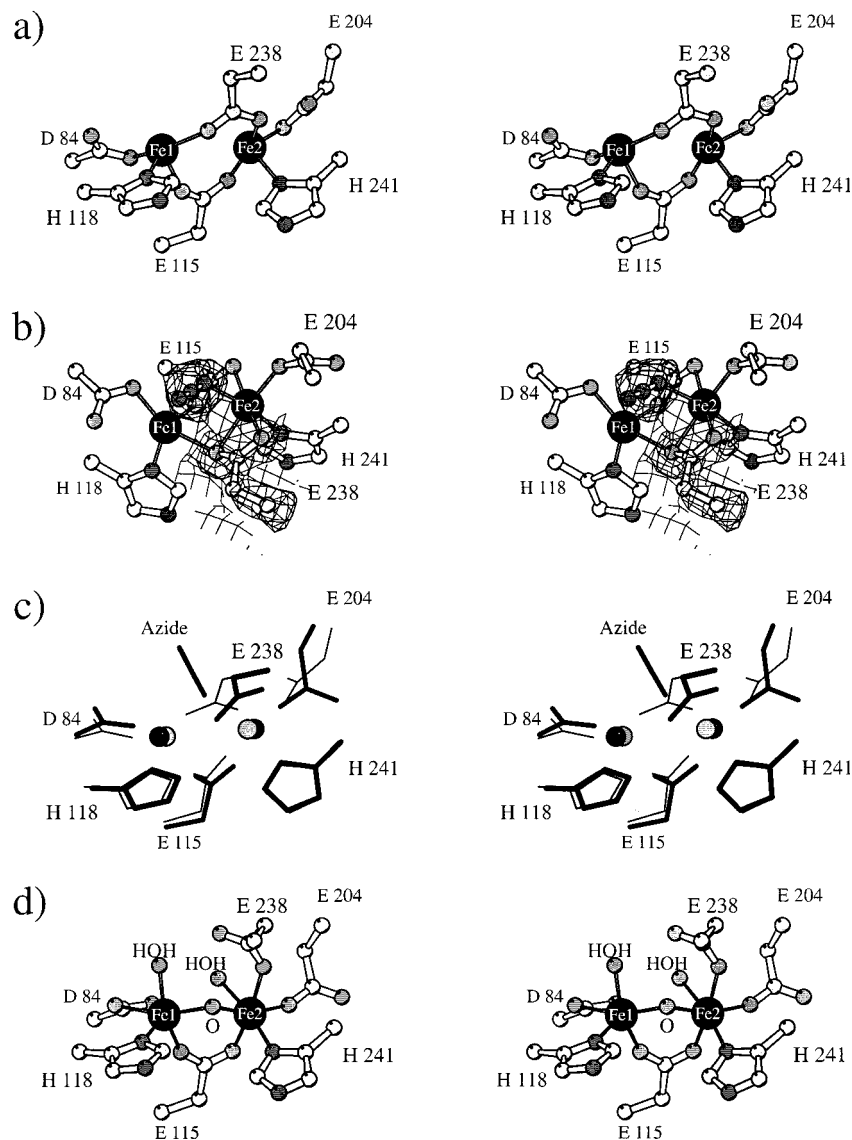
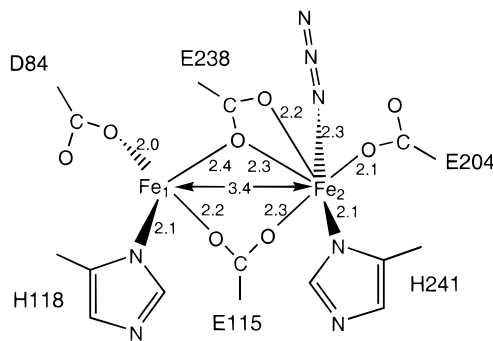


**Figure 1.** (a, b) Stereoview of the residues around the Fe-center in the two azide soaked structures: (a) Reduced wt-protein soaked in azide; (b) Reduced F208A/Y122F complexed with azide. An omit map for the azide molecule and a 2Fo-Fc map for E238 are shown. (c) Overlay of the reduced wt-protein and the reduced F208A/Y122F-azide complex. (d) Met form of the wt-protein. This figure was generated with BOBSCRIPT,<sup>61</sup> a modification of MOLSCRIPT.<sup>62</sup>

In the structure of the reduced F208A/Y122F protein soaked in azide, at the same conditions as wt R2, it is clear that azide binds in an ordered manner to the Fe-center, seen as a clear positive elongated peak in the Fo-Fc maps into which an azide molecule could easily be modeled (Figure 1b). This density was present only in the A subunit in accordance with previous observations that diffusion into the B subunit is restricted in this crystal form.<sup>45</sup> Therefore we also obtained the structure of the uncomplexed reduced F208A/Y122F protein in the B subunit, which revealed that the two mutations in this protein had no significant effect on the structure of the Fe-center. In the refined azide complex in the A subunit the azide molecule coordinates in an  $\eta^1$ -terminal fashion to Fe2 with a coordination distance of 2.3 Å (Figure 1b and Scheme 2). There is also a change in coordination number on Fe2, which becomes 6-coordinate. The most interesting change that occurs apart from the azide binding is the carboxylate shift seen for residue E238. The E238 adopts a new  $\mu$ -( $\eta^2, \eta^1$ ) bridging conformation where one carboxylate oxygen is bridging the two Fe atoms at distances of 2.4 and 2.3 Å to Fe1 and Fe2, respectively. The second carboxylate oxygen of E238 is coordinated to Fe2 at a distance

**Scheme 2.** Metal-Ligand Distances in the Azide Complexed F208A/Y122F Protein



of 2.2 Å. This is a new conformation of this residue that has not been seen in any previous crystal structures of the R2 protein. Furthermore, the Fe-Fe distance is significantly shorter in this structure than is usually found in reduced R2 structures (Figure 1c), 3.4 Å in the azide complex as opposed to 3.8 Å in normal reduced R2. This shorter Fe-Fe distance is probably due to the extra bridging oxygen of E238. It should be noted

that the bridging oxygen from E238 takes the place of the  $\mu$ -oxo bridge in the structure of the met R2 protein (Figure 1d).

In the wt-protein no azide binding could be detected. The fact that azide was not visible in our electron density maps suggests that, if azide binds to the Fe-center, it has to bind in a disordered fashion or at low occupancy at the conditions used. EPR and MCD studies show some binding of azide to wt diferrous *E. coli* R2 in solution with two different affinity constants with  $K_d$  of 30–70 and 330 mM,<sup>37</sup> while mouse R2 show azide interaction with a single  $K_d$  around 40–50 mM.<sup>38</sup> The iron center in mouse R2<sup>48</sup> is more open than *E. coli* wt and its azide binding properties might be more similar to the F208A/Y122F mutant. The observed structure in the F208A/Y122F azide complex includes a single bridging carboxylate oxygen from E238, and this bridging oxygen corresponds well to the weak ferromagnetic coupling observed by EPR, MCD, and saturation magnetization measurements of the mouse<sup>38</sup> and *E. coli*<sup>36,37</sup> R2 in the presence of 0.5 M azide. A bridging oxygen atom on E238 has been proposed as one possible explanation for the stronger coupling between the Fe ions induced by azide binding,<sup>37</sup> but it could not be definitively concluded. Thus, the observed structure of the azide complex of F208A/Y122F explains very well the magnetic data from both wt *E. coli* and wt mouse R2 and is also in agreement with the change in coordination number and the change in zero field splitting parameters of the Fe-center.

**Structure of the Oxidized F208A/Y122F Protein.** The larger hydrophobic pocket formed by the removal of the F208 side chain in the F208A/Y122F mutant does not perturb the rest of the protein structure in any significant way and leaves an “active site” pocket of similar size as the one found in MMO. The coordination environment of the Fe-center remains unchanged compared to the oxidized wt-protein. This mutation, in combination with other mutations around the Fe-center, may become a very useful model system to study hydroxylation chemistry in this class of proteins.

**Comparison with Other Structures of Azide Complexes of Iron Proteins.** One complex of another diiron protein with azide previously characterized by X-ray crystallography is the azide complex of diferric (met) hemerythrin.<sup>49,50</sup> In this case azide binds terminally to one of the iron ions in the same position as the oxygen molecule in oxy-Hr. Comparison between hemerythrin and R2 is complicated by the fact that the redox state and coordination environment in the two proteins are different. Studies have been performed on Fe-porphyrin proteins where azide is found to bind the ferrous state in a manner similar to dioxygen.<sup>51,52</sup> Both these cases support the use of azide as a model for the binding of dioxygen. Other X-ray crystallographic studies of azide complexes of proteins more related to R2 have not been performed.

**Mechanistic Implications.** In the F208A/Y122F mutant the azide molecule is bound in an  $\eta^1$ -terminal mode to Fe2. This may be of relevance to the reaction mechanism since this mode of binding could reflect the initial binding of dioxygen. The

most interesting feature of this structure is the shift in bridging mode seen in the E238 residue where one of the carboxylate oxygens becomes a bridging ligand while the other oxygen retains its coordination to Fe2. Strangely this residue has been ignored in most previous discussions on the mechanism of diiron oxygen proteins. We believe that this new carboxylate shift of E238 could be a key feature for understanding the oxygen activation mechanism at this kind of Fe-center. We have therefore outlined a detailed reaction mechanism (Figure 2a) based on our azide structure, spectroscopic data on intermediate X, and the following three assumptions: (I) The E238 retains its new bridging conformation throughout the oxygen activation reaction. (II) No protein- or dioxygen-derived ligands leave the coordination sphere during the reaction. (III) The Fe ions will never have a coordination number higher than 6.<sup>53</sup>

The first two assumptions are based on the expectation that the charge build-up on the iron ions during the reaction is unlikely to promote the release of coordinating polar ligands. The shift in the E238 residue seen in the F208A/Y122F azide structure would, in contrast to previously discussed mechanisms, restrict the outcome of dioxygen cleavage toward the asymmetric structure for intermediate X as proposed from spectroscopic studies. The above assumptions and hence the suggested mechanism could also be true for the MMO system. We suggest that, starting from the diferrous center, dioxygen bind in a terminal fashion to Fe2, in the position of azide in our F208A/Y122F structure. The next intermediate in the cycle is the peroxo form that has been detected in MMO<sup>27</sup> and recently in the D84E mutant of R2.<sup>54</sup> The structure proposed here for the peroxo form would render the Fe2 ion coordinatively saturated by protein- and dioxygen-derived ligands and in the subsequent oxygen cleavage reaction leave one coordination position free on Fe1. This would steer the outcome of the dioxygen cleavage reaction to a defined stereochemistry and direct the terminal, reactive oxo/hydroxo ligand of X to Fe1. We suggest the terminal oxygen species on Fe1 to be the key reactive group on the activated diiron site. This is consistent with Fe1 being closest to the substrate tyrosine in the R2 case. Another fact in favor of this suggestion is that if a highly reactive oxygen species is formed at the free coordination site on Fe1 it would point toward a small hydrophobic pocket made up mainly by the invariant residue I234 in R2, a residue that is conserved in all R2 and  $\Delta^9$  desaturase sequences.

Our conclusion that E238 is a key player in controlling the oxygen activation is further corroborated by the structure of the oxidized E238A/Y122F mutant, which has been determined recently.<sup>55</sup> This structure revealed that hydroxylation chemistry occurs in this mutant and residue F208 becomes hydroxylated at the meta position during the reaction with dioxygen. The phenolic oxygen formed ends up being coordinated to Fe2. This has not been seen in other R2 mutants where the Y122 and/or residues in the proton/electron-transfer pathway have been removed.

If we extrapolate the above suggestions regarding the mechanism in R2 to the MMO system, we also find some

(48) Kauppi, B.; Nielsen, B. A.; Ramaswamy, S.; Larsen, I. K.; Thelander, M.; Thelander, L.; Eklund, H. *J. Mol. Biol.* **1996**, *262*, 706–720.

(49) Stenkamp, R. E.; Seiker, L. C.; Jensen, L. H. *J. Mol. Biol.* **1978**, *126*, 457–466.

(50) Holmes, M. A.; Stenkamp, R. E. *J. Mol. Biol.* **1991**, *220*, 723–737.

(51) Tarricone, C.; Galazzi, A.; Coda, A.; Ascenzi, P.; Bolognesi, M. *Structure* **1997**, *5*, 497–507.

(52) Conti, E.; Moser, C.; Rizzi, M.; Mattevi, A.; Lionetti, C.; Coda, A.; Ascenzi, P.; Brunori, M.; Bolognesi, M. *J. Mol. Biol.* **1993**, *233*, 498–508.

(53) There are reports of seven-coordinate Fe ions in the literature, but these usually involve ligand molecules with high covalent rigidity to place five of the ligating atoms in one plane.<sup>59,60</sup> In the protein, steric effects would make it difficult to accommodate seven ligands to any of the Fe ions. Furthermore, seven-coordinate Fe ions have never been proposed to be involved in these reactions.

(54) Bollinger, J. M.; Krebs, C.; Vicol, A.; Chen, S.; Ley, B. A.; Edmondson, D. E.; Huynh, B. H. *J. Am. Chem. Soc.* **1998**, *120*, 1094–1095.

(55) Logan, D. T.; deMaré, F.; Persson, B. O.; Slaby, A.; Sjöberg, B.-M.; Nordlund, P. *Biochemistry* **1998**, *37*, 10798–10807.

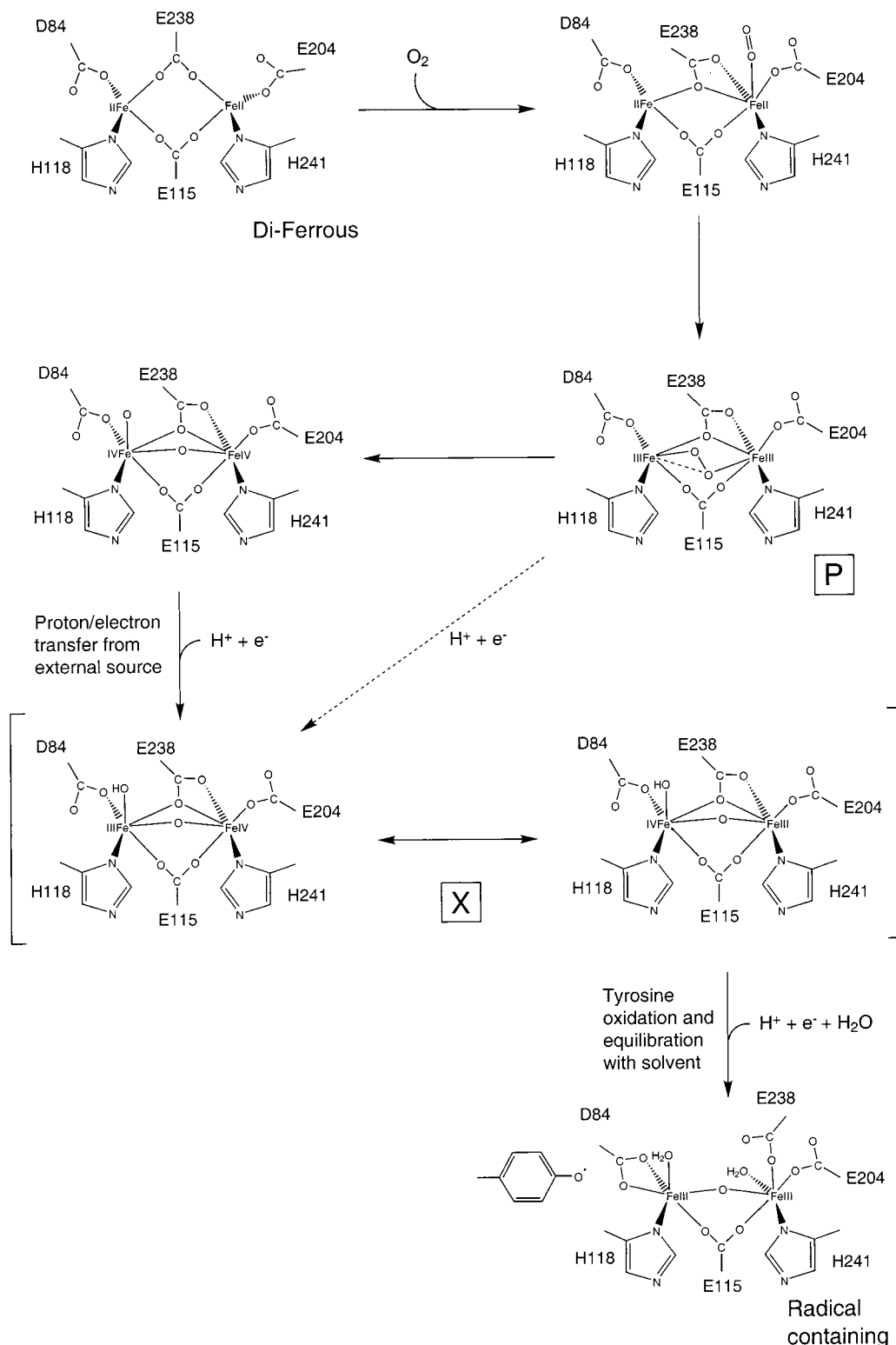


**Figure 2.** Proposed detailed mechanism of diiron-catalyzed dioxygen activation. Boxed letters indicate experimentally studied intermediates. According to our proposal, oxygen binding induces the conformational change in E238 rendering Fe2 6-coordinate. Two electrons are transferred from the Fe-center to dioxygen to yield bound peroxide and a diferric Fe-center. Both Fe ions, from the peroxide form and onward, are 6-coordinate. From the peroxide form (P), further cleavage of the O–O bond gives one bridging and one terminal oxo group and a formally diferryl center. O–O bond cleavage is rapidly followed by, or concurrent with (dashed arrow), proton/electron transfer via the radical transfer pathway (Scheme 1) to yield intermediate X. Only very small positional changes of the two oxygen atoms as well as of the protein-derived ligands are required throughout the reaction.

interesting points. In the case of MMO the cleavage of the oxygen molecule leads to the formation of an intermediate termed Q containing a (Fe<sup>IV</sup>)<sub>2</sub> species.<sup>28</sup> On the basis of the structural similarities between MMO and R2 and a recent observation that Q in MMO and X in R2 are similar<sup>56</sup> we

suggest that the formation of this species is steered in this reaction by E243 (the equivalent of E238 in R2) in a manner

(56) Valentine, A. M.; Tavares, P.; Pereira, A. S.; Davydov, R.; Krebs, C.; Hoffman, B. M.; Edmondson, D. E.; Huynh, B. H.; Lippard, S. J. *J. Am. Chem. Soc.* **1998**, *120*, 2190–2191.

similar to the R2 reaction. This postulates the formation of a terminal Fe<sup>IV</sup>-coordinated oxo group on Fe1 and that both iron ions at the stage of Q are 6-coordinate with no coordination positions free to coordinate water or to form the proposed Fe—C bond.<sup>57,58</sup>

In conclusion, the details of the mechanism for the dioxygen cleavage reaction in diiron proteins presented here are new and unique in that we have suggested possible detailed conformations of all Fe ligands for all observed intermediates. The proposed structures appear to be in good agreement with earlier structural and spectroscopic data and with the placement of the intermediates in their structural context in the protein. Furthermore, an attractive point of this reaction pathway is that it requires very small conformational changes after the oxygen molecule is bound to the Fe-center. This would be consistent with the rapid kinetics seen for these reactions and would be advantageous for controlling the reactive oxygen species during the reaction to prevent destructive side reactions. This is a key point for the evolution of biologically successful chemical mechanisms. The assumptions that E238 in R2 and E243 in MMO retain their  $\mu$ -( $\eta^2, \eta^1$ ) bridged conformation throughout the O<sub>2</sub> activation and that no protein-derived ligands leave the

(57) Barton, D. H. R.; Beck, A. H.; Taylor, D. K. *Tetrahedron* **1995**, *81*, 5245–5254.

(58) Siegbahn, P. E. M.; Crabtree, R. H. *J. Am. Chem. Soc.* **1997**, *119*, 3103–3113.

(59) Vasilevsky, I.; Rose, N. J.; Stenkamp, R. E. *Acta Crystallogr. B* **1992**, *48*, 444–449.

(60) Zhang, D.; Busch, D. H.; Lennon, P. L.; Weiss, R. H.; Neumann, W. L.; Riley, D. P. *Inorg. Chem.* **1998**, *37*, 956–963.

(61) Esnouf, R. M. *J. Mol. Graph.* **1997**, *15*, 133–138.

(62) Kraulis, P. J. *J. Appl. Crystallogr.* **1991**, *24*, 946–950.

coordination sphere during the reaction, in combination with consideration of the possible coordination modes for Fe ions, in effect restrict the possible structures for the different intermediates to *only* the ones outlined in this report. Furthermore, the mechanism proposed here excludes the presence of coordinating waters during the reaction, and although the present study gives a likely scenario for the dioxygen cleavage reaction, more detailed studies of the intermediates involved are required to corroborate this hypothesis. However, if the structures of the high-valent intermediates presented here are correct, they significantly restrict the possible structures of the species involved in the substrate oxidation steps of these reactions. The very detailed structures of the different intermediates presented here can now be directly used to simulate spectra for EPR, ENDOR, and EXAFS data obtained for the various intermediates and serve as a basis for theoretical calculations to test our hypothesis.

**Acknowledgment.** This work was supported by grants from the Swedish Research Council for Engineering Sciences (TFR) to P.N. and B.-M. S., the Swedish Research Council for Natural Sciences (NFR) to P. N., the Research Council of Norway to K.K.A., the EU CONTRACT No. FMRX-CT98-0207 (Iron–oxygen protein network), and the Research Council of Norway to the Synchrotron user group in Oslo (SYGOR). We are grateful to Dr. K. Knudsen for help at the Swiss–Norwegian beam line at the ESRF and Agneta Slaby for preparation of the wt R2 protein.

JA982280C